Progressive Bitstream Optimization in MIMO Channels Based on a Comparison Between OSTBC and SM

Seok-Ho Chang†, Pamela C. Cosman‡ and Laurence B. Milstein‡
†MSE Dept. Dankook University, Yongin, South Korea
‡ECE Dept. University of California at San Diego, La Jolla, CA 92093, USA

***Abstract*—We study the optimal design of the multimedia communication systems that employ open-loop multiple-input multiple-output (MIMO) techniques. We first analyze the behavior of the crossover point of the error probability curves for orthogonal space-time block codes (OSTBC) and spatial multiplexing (SM) with a zero-forcing receiver. It is proven that in the high signal-to-noise ratio (SNR) regime, for both the information outage probability and the uncoded bit error rate, as data rate increases, the crossover point for the error probability monotonically decreases, and the crossover point for the SNR monotonically increases. Those results can be exploited for the optimal transmission of multimedia progressive sources which need unequal target error rates or transmission data rates in their bitstream; we show that the computational complexity involved with the optimal space-time coding of a progressive bitstream can be simplified.**

I. Introduction

The increasing demand for multimedia services has motivated much research on cross-layer design [1], [2]. Multimedia progressive sources such as embedded image or scalable video [3], [4] employ a mode of transmission such that as more bits are received, the source can be reconstructed with better quality. However, these advances in source codecs have also rendered the encoded bitstreams very sensitive to channel impairments. Multiple-input multiple-output (MIMO) channels are able to provide performance gains in terms of reliability and transmission rate [5][6].

In this paper, we study the optimal design of a low-complex MIMO system for the transmission of multimedia progressive sources. We first compare OSTBC and SM from the viewpoint of their error probabilities. Our approach focuses on how the crossover point of the error probability curves for the space-time codes behaves in the high SNR regime. In some literature, the crossover point of the ergodic capacity curves has been investigated [7], [8]. On the other hand, we compare error probabilities, such as information outage probability and uncoded bit error rate (BER), of OSTBC and SM in an analytic manner for arbitrary numbers of antennas. Note that some results for the uncoded BER with two tranmit antennas were presented in [9] by the authors.

We prove that as data rate increases, the crossover point in error probability monotonically decreases, whereas that in the SNR monotonically increases; these results are strictly proven for arbitrary numbers of transmit and receive antennas, and the spatial multiplexing rate of OSTBC. Regarding SM, our analysis is focused on a ZF linear receiver, in part since the joint probability distribution of the post-processing SNRs for that receiver is properly characterized such that error probability can be obtained in a closed form. Note that novel wireless communication systems are targeting very large spectral efficiencies [10], and the use of low-complexity linear receivers may be mandatory because of complexity and power consumption.

We exploit the above analytical results for the optimal space-time coding of multimedia progressive sources. The progressive sources have a significant feature that they have steadily decreasing importance for bits later in the stream, which makes unequal target error rates useful. Our analysis for the crossover point is used to optimally assign OSTBC or SM techniques to each portion of the progressive bitstream to be transmitted over Rayleigh fading channels.

II. System Model

Consider a MIMO system with N_t transmit and N_r receive antennas in a frequency flat-fading channel. A space-time codeword $\mathbf{S} = [\mathbf{s}_1 \cdots \mathbf{s}_T]$ of size $N_t \times T$ is transmitted over T symbol durations via N_t transmit antennas. At the kth time symbol duration, we have

$$\mathbf{y}_k = \mathbf{H}\mathbf{s}_k + \mathbf{n}_k, \qquad k = 1, \cdots, T \tag{1}$$

where $\mathbf{y}_k$ is the $N_r \times 1$ received signal vector, $\mathbf{H}$ is the $N_r \times N_t$ channel matrix, and $\mathbf{n}_k$ is a $N_r \times 1$ zero mean complex Gaussian vector with $\mathcal{E}\left[\mathbf{n}_k\mathbf{n}_l^H\right]=\sigma_n^2\mathbf{I}_{N_r}\delta(k-l)$, where $(\cdot)^H$ denotes the Hermitian operation. We assume that the entries of $\mathbf{H}$ are independent and identically distributed (i.i.d) $\sim \mathcal{CN}(0,1)$, and that $\mathbf{H}$ is random but constant over the duration T of a codeword. Let $\gamma_s := \mathcal{E}\left[|(\mathbf{s}_k)_i|^2\right]/\sigma_n^2$ denote SNR per symbol, where $(\mathbf{s}_k)_i$ is the ith component of the transmit signal vector $\mathbf{s}_k$ ($i = 1, \cdots, N_t$). Let N_s denote the number of symbols packed within a space-time codeword $\mathbf{S}$. The spatial multiplexing rate is defined as N_s/T. We assume no channel state information (CSI) at the transmitter, and perfect CSI at the receiver.

III. The Behavior of the Crossover Points of the Error Probability Curves

A. Average Uncoded BER

We first express the BER of the OSTBC for an M-ary square QAM constellation. A closed-form expression for the BER of SISO systems in an AWGN channel is given by [11, Eq. (14)]. For OSTBC, the same constellation symbol,

978-0-7695-5124-1/13 $31.00 © 2013 IEEE
DOI 10.1109/MILCOM.2013.99

$(\mathbf{s}_k)_i$, is transmitted N_t times during T symbol durations; thus, for an M-ary QAM, the SNR per bit, γ_b, is given by $\gamma_b = N_t \times \gamma_s / \log_2 M$. The post-processing SNR per symbol is given by $\gamma_s \|\mathbf{H}\|_F^2$, where $\|\cdot\|_F$ denotes the Frobenius norm. From these, it can be readily shown that the exact BER of the OSTBC for an M-ary square QAM is given by

$$P_{b,OSTBC} = \frac{4}{\sqrt{M}\log_2 M} \sum_{k=1}^{\log_2 \sqrt{M}} \sum_{i=0}^{(1-2^{-k})\sqrt{M}-1} \left[(-1)^{\left\lfloor \frac{i \cdot 2^{k-1}}{\sqrt{M}} \right\rfloor} \left(2^{k-1} - \left\lfloor \frac{i \cdot 2^{k-1}}{\sqrt{M}} + \frac{1}{2} \right\rfloor \right) \left(\frac{1-\mu(i)}{2} \right)^{N_t N_r} \times \sum_{j=0}^{N_t N_r - 1} \left\{ \binom{N_t N_r - 1 + j}{j} \left(\frac{1+\mu(i)}{2} \right)^j \right\} \right] \quad (2)$$

where

$$\mu(i) = \sqrt{\frac{3(2i+1)^2 (\log_2 M) \gamma_b}{2N_t(M-1) + 3(2i+1)^2 (\log_2 M) \gamma_b}}.$$

We next present the BER of the SM scheme. For a ZF receiver, the post-processing SNR on each substream is a chi-square random variable, and thus the exact BER expression is achievable. The BER of SM with a ZF receiver for an M-ary QAM, denoted by $P_{b,SM-ZF}$, is given by [12, Eq. (3.12)].

In the following, we find the crossover point of the BER curves of OSTBC and SM with a ZF receiver. The BER expressions given by (2) and [12, Eq. (3.12)] are polynomials in γ_b with degrees greater than four, even for the simplest case of a 2×2 channel matrix. For these equations, there exists no closed-form solution for the crossover point. Thus, we will explore the asymptotic regime of high SNR; if we discard the error function terms having non-minimum Euclidian distances, and use $\sqrt{\frac{x}{1+x}} \approx 1 - \frac{1}{2x}$ for $x >> 1$, we have

$$P_{b,OSTBC} \approx P_{b,OSTBC}^{app} = \binom{2N_t N_r - 1}{N_t N_r} \times \frac{4(\sqrt{M}-1)}{\sqrt{M}\log_2 M} \left(\frac{N_t(M-1)}{6\log_2 M} \right)^{N_t N_r} \left(\frac{1}{\gamma_b} \right)^{N_t N_r}. \quad (3)$$

In the same way, $P_{b,SM-ZF}$ is approximated as [12, Eq. (3.19)]. We compare the BERs of OSTBC and SM under the condition that the transmission data rates of both are set to be equal. To do this, we employ m-ary QAM for the SM, and m^{N_t/r_s}-ary QAM for the OSTBC, where $0 < r_s \le 1$ denotes the spatial multiplexing rate of the OSTBC. We assume that $m \ge 4$ (i.e., QPSK), and $N_r \ge N_t \ge 2$. We let $M = m^{N_t/r_s}$ in (3), and let $M = m$ in [12, Eq. (3.19)]. Then, we find the SNR, γ_b^*, for which the two resultant equations are equal. It can be shown that γ_b^* is given by

$$\gamma_b^* = \left(\frac{\binom{2N_t N_r - 1}{N_t N_r} r_s^{N_t N_r + 1} \sqrt{m}}{\binom{2(N_r - N_t)+1}{N_r - N_t + 1} 6^{(N_r+1)(N_t-1)} N_t (\sqrt{m}-1) m^{N_t/2r_s}} \times \frac{(m^{N_t/2r_s} - 1)(m^{N_t/r_s} - 1)^{N_t N_r}}{(\log_2 m)^{(N_r+1)(N_t-1)} (m-1)^{N_r - N_t + 1}} \right)^{\frac{1}{(N_r+1)(N_t-1)}} \quad (4)$$

We define the function $f(m)$ as

$$f(m) = \frac{\sqrt{m}(m^{N_t/r_s} - 1)}{(\sqrt{m}-1)(m-1)} \cdot \frac{m^{N_t/2r_s} - 1}{m^{N_t/2r_s}} \times \left(\frac{m^{N_t/r_s} - 1}{m-1} \right)^{N_t N_r - 1} \left(\frac{m-1}{\log_2 m} \right)^{(N_r+1)(N_t-1)}. \quad (5)$$

It can be proven that $f(m)$ is a strictly increasing function in m, under the condition that $m \ge 4$, $N_r \ge N_t \ge 2$, and $0 < r_s \le 1$.[1] From (4) and (5), it has been shown that as the alphabet size, m, increases, γ_b^* strictly increases, regardless of the numbers of transmit and receive antennas, and the spatial multiplexing rate of the OSTBC. If we substitute both γ_b^*, given by (4), and $M = m^{N_t/r_s}$ into (3), the corresponding BER, P_b^*, is given by

$$P_b^* = \frac{4 r_s^{N_t N_r + 1}}{N_t} \binom{2N_t N_r - 1}{N_t N_r} \left(\frac{N_t \binom{2(N_r - N_t)+1}{N_r - N_t + 1}}{r_s^{N_t N_r + 1} \binom{2N_t N_r - 1}{N_t N_r}} \right)^{\frac{N_t N_r}{(N_r+1)(N_t-1)}} \times \left(\frac{(\sqrt{m}-1) m^{N_t/2r_s}}{\sqrt{m}(m^{N_t/2r_s} - 1)} \right)^{\frac{N_t N_r}{(N_r+1)(N_t-1)}} \times \frac{m^{N_t/2r_s} - 1}{m^{N_t/2r_s} \log_2 m} \left(\frac{m-1}{m^{N_t/r_s} - 1} \right)^{\frac{N_t N_r (N_r - N_t + 1)}{(N_r+1)(N_t-1)}}. \quad (6)$$

It can also be proven that P_b^* is a strictly decreasing function in m. That is, as the alphabet size, m, increases, P_b^* strictly decreases, for an arbitrary number of transmit and receive antennas, and the spatial multiplexing rate of OSTBC. Further, from (3) and [12, Eq. (3.19)], it can be shown that

$$P_{b,OSTBC}^{app} < P_{b,SM-ZF}^{app} \quad \text{for} \quad \gamma_b > \gamma_b^*,$$
$$P_{b,OSTBC}^{app} > P_{b,SM-ZF}^{app} \quad \text{for} \quad \gamma_b < \gamma_b^*. \quad (7)$$

Let $P_{b,1}^*$ and $\gamma_{b,1}^*$ denote the crossover point when a modulation alphabet size $m = M_1$ is employed, and $P_{b,2}^*$ and $\gamma_{b,2}^*$ denote the crossover point when an alphabet size $m = M_2$ is used. Suppose that $M_1 < M_2$. Then, from the results above, we have

$$\gamma_{b,1}^* < \gamma_{b,2}^* \quad \text{and} \quad P_{b,1}^* > P_{b,2}^*. \quad (8)$$

B. Information Outage Probability

The information outage probability of the OSTBC is given by [14]

$$P_{out,OSTBC} = P\left[r_s \log_2 \left(1 + \frac{\gamma_s}{r_s} \|\mathbf{H}\|_F^2 \right) < R \right] \quad (9)$$

where R is the transmission data rate (bits/s/Hz). Using the cumulative density function (CDF) of $\|\mathbf{H}\|_F^2$, which is a chi-square random variable with $2N_t N_r$ degrees of freedom, it can be shown that

$$P_{out,OSTBC} = 1 - \exp\left(-\frac{r_s}{\gamma_s} \left(2^{R/r_s} - 1 \right) \right) \times \sum_{k=1}^{N_t N_r} \frac{1}{(k-1)!} \left(\frac{r_s}{\gamma_s} \left(2^{R/r_s} - 1 \right) \right)^{k-1}. \quad (10)$$

[1]The detailed steps of all the analysis in Section III can be found in [13].

For the SM scheme, we consider pure spatial multiplexing where data is split into several substreams, one for each transmit antenna, and each substream undergoes independent temporal coding to avoid a complex joint decoding of substreams at the receiver. For this scheme, an outage event occurs when any of the subchannels cannot support the data rate assigned to it. Thus, the information outage probability is given by [10]

$$P_{out,SM-ZF} = P\left[\bigcup_{k=1}^{N_t}\left\{\log_2\left(1+\gamma_s\eta_k\right) < \frac{R}{N_t}\right\}\right] \quad (11)$$

where η_k is a chi-square random variable with $2(N_r - N_t + 1)$ degrees of freedom ($k = 1, \cdots, N_t$). Based on the assumption that η_k's are independent for a ZF receiver [15], and using the CDF of a chi-square random variable, it can be shown that

$$P_{out,SM-ZF} = 1 - \left[\exp\left(-\frac{1}{\gamma_s}\left(2^{R/N_t}-1\right)\right) \times \sum_{k=1}^{N_r-N_t+1}\frac{1}{(k-1)!}\left(\frac{1}{\gamma_s}\left(2^{R/N_t}-1\right)\right)^{k-1}\right]^{N_t}. \quad (12)$$

Next, we will find the crossover point of the outage probability curves of OSTBC and SM with a ZF receiver. Since the expressions given by (10) and (12) are not analytically tractable, to obtain a closed-form solution of the crossover point, we consider high SNR approximate expressions; if we use only the dominant terms in the numerator and denominator of the Taylor series expansion of (10), we have

$$P_{out,OSTBC} \approx P_{out,OSTBC}^{app} = \frac{1}{(N_tN_r)!}\left(\frac{r_s}{\gamma_s}\left(2^{R/r_s}-1\right)\right)^{N_tN_r}. \quad (13)$$

For the SM scheme, the high SNR approximate expression is given by [15]

$$P_{out,SM-ZF} \approx P_{out,SM-ZF}^{app} = \frac{N_t}{(N_r-N_t+1)!}\left(\frac{1}{\gamma_s}\left(2^{R/N_t}-1\right)\right)^{N_r-N_t+1}. \quad (14)$$

We find the SNR, γ_s^*, for which (13) and (14) are the same:

$$\gamma_s^* = \left(\frac{(N_r-N_t+1)!\; r_s^{N_tN_r}\;(2^{R/r_s}-1)^{N_tN_r}}{(N_tN_r)!\; N_t\;(2^{R/N_t}-1)^{N_r-N_t+1}}\right)^{\frac{1}{(N_r+1)(N_t-1)}} \quad (15)$$

It can be proven that γ_s^* is a strictly increasing function in R, under the condition that $R > 0$, $N_r \geq N_t \geq 2$, and $0 < r_s \leq 1$. If we substitute γ_s^* into (13), the corresponding outage probability, P_{out}^*, is given by

$$P_{out}^* = \frac{r_s^{N_tN_r}}{(N_tN_r)!}\left(2^{R/r_s}-1\right)^{N_tN_r}\left(\frac{(N_tN_r)!\; N_t}{(N_r-N_t+1)!\; r_s^{N_tN_r}} \times \frac{(2^{R/N_t}-1)^{N_r-N_t+1}}{(2^{R/r_s}-1)^{N_tN_r}}\right)^{\frac{N_tN_r}{(N_r+1)(N_t-1)}}. \quad (16)$$

It can also be proven that P_{out}^* is a strictly decreasing function in R. Hence, as the transmission data rate, R, increases, γ_s^* strictly increases and P_{out}^* strictly decreases, regardless of the numbers of transmit and receive antennas, and the spatial multiplexing rate of OSTBC. Further, from (13) and (14), it can be shown that

$$P_{out,OSTBC}^{app} < P_{out,SM-ZF}^{app} \text{ for } \gamma_s > \gamma_s^*, \quad P_{out,OSTBC}^{app} > P_{out,SM-ZF}^{app} \text{ for } \gamma_s < \gamma_s^*. \quad (17)$$

Let $P_{out,1}^*$ and $\gamma_{s,1}^*$ denote the crossover point when a transmission data rate $R = R_1$ is employed, and $P_{out,2}^*$ and $\gamma_{s,2}^*$ denote the crossover point when a data rate $R = R_2$ is used. Suppose that $R_1 < R_2$. Then, from the results above, we have

$$\gamma_{s,1}^* < \gamma_{s,2}^* \quad \text{and} \quad P_{out,1}^* > P_{out,2}^*. \quad (18)$$

Based on (17) and (18), the high SNR approximate outage probabilities of OSTBC and SM with a ZF receiver are qualitatively depicted in Fig. 1. For data rate $R_1 < R_2$, in Fig. 1, the outage probabilities have the following properties: i) $\gamma_{s,1}^* < \gamma_{s,2}^*$ ii) $P_{out,1}^* > P_{out,2}^*$ iii) $P_{out,i,OSTBC}^{app} < P_{out,i,SM-ZF}^{app}$ for $\gamma_{s,i} > \gamma_{s,i}^*$, and $P_{out,i,OSTBC}^{app} > P_{out,i,SM-ZF}^{app}$ for $\gamma_{s,i} < \gamma_{s,i}^*$ $(i = 1, 2)$. Suppose that a target outage probability, $P_{out,T}$, is smaller than $P_{out,1}^*$ but greater than $P_{out,2}^*$. Then, from Fig. 1, it is seen that OSTBC is preferable to SM for a data rate R_1, whereas SM is preferable for a data rate R_2. Note that the results for the uncoded BER, given by (7) and (8), are coincidentally analogous to those for the information outage probability, given by (17) and (18). Hence, the same argument above can be made for the uncoded BER.

IV. Optimal Space-Time Coding for the Progressive Sources

The analysis in the previous section can be exploited to optimally design a low complex MIMO system for the transmission of the applications which require need unequal target error rates or transmission data rates in their bitstream. In the following, we present the transmission of multimedia progressive sources [3], [4].

Progressive encoders employ progressive transmission so that encoded data have gradual differences of importance in their bitstreams. Suppose that the system takes the bitstream from the progressive source encoder, and transforms it into a

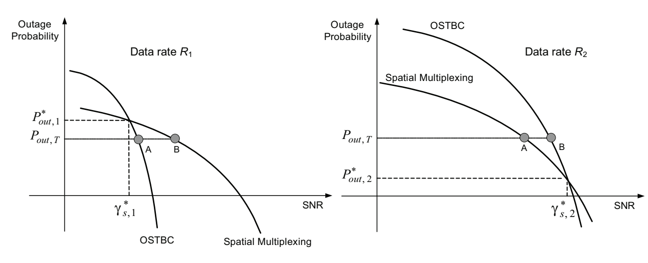

Fig. 1. High SNR approximate outage probabilities of OSTBC and SM with a ZF receiver for the same transmission data rates.

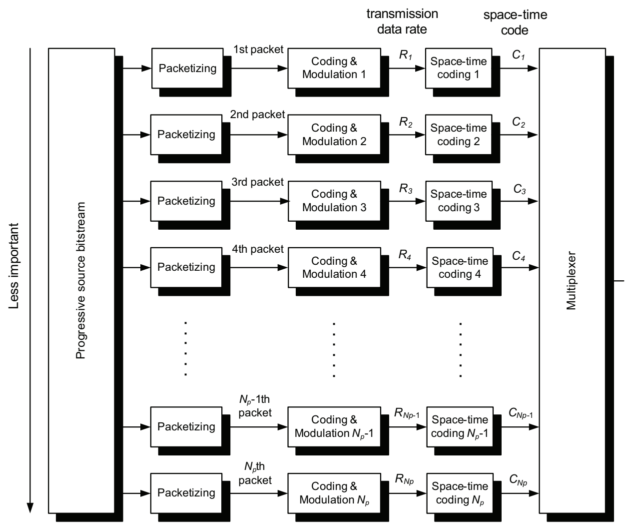

Fig. 2. Progressive source transmission system combined with open-loop MIMO techniques. R_i and C_i denote the transmission data rate and the space-time code assigned to ith packet, respectively ($1 \leq i \leq N_P$).

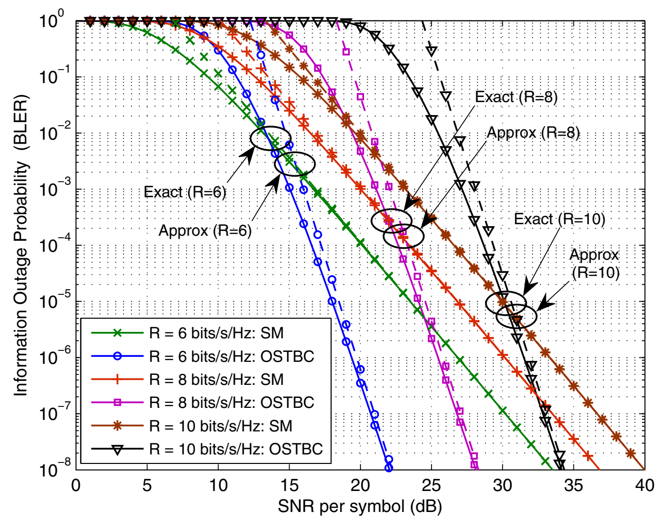

Fig. 3. The exact and high SNR approximate outage probabilities of OSTBC and SM with a ZF receiver for 2×4 MIMO systems in i.i.d Rayleigh fading channels. Solid curves denote the exact outage probabilities, and dashed curves denote the high SNR approximate outage probabilities. The exact and approximate crossover points are marked with circles.

sequence of N_P packets. Such a system is depicted in Fig. 2. Each of these N_P progressive packets can be encoded with different transmission data rates, as well as different MIMO techniques, so as to yield the best end-to-end performance as measured by the expected distortion of the source. The error probability of an earlier packet needs to be lower than or equal to that of a later packet, due to the gradually decreasing importance in the progressive bitstream. Thus, given the same transmission power, the earlier packet requires a transmission data rate which is lower than or equal to that of the later packet.

Let N_R denote the number of candidate transmission data rates employed by a system. The number of possible assignments of N_R data rates to N_P packets would exponentially grow as N_P increases. Further, in a MIMO system, if each packet can be encoded with different space-time codes (e.g., OSTBC or SM in this case), the assignment of space-time codes as well as data rates to N_P packets yields a more complicated optimization problem, compared to a SISO system. Note that each source, e.g., an image, has its inherent rate-distortion characteristic, from which the performance of the expected distortion is computed. Hence, for example, when a series of images is transmitted, the above optimization should be addressed in a real-time manner, considering which specific image (i.e., rate-distortion characteristic) is transmitted in the current time slot.

For a MIMO system, we use the analytical results presented in the previous section to optimize the assignment of space-time codes to progressive packets. Recall that, for a progressive source, the error probability of an earlier packet needs to be lower than or equal to that of a later packet, and the earlier packet requires a transmission data rate which is lower than or equal to that of the later packet. Suppose that the kth packet in a sequence of N_P packets is encoded with SM. Then, our analysis tells us that the $k+1$st, $k+2$nd, $\ldots$, N_Pth packets also should be encoded with SM rather than with OSTBC. This is because we have proven that, when SM is preferable for a packet with a transmission data rate of R_1, a packet with a data rate of $R_2 (> R_1)$ also should be encoded with SM, as long as the target error rate of the latter is the same as or higher than that of the former (Fig. 1 can be referred to). As a result, it can be shown that the number of possible assignments of space-time codes to N_P packets can be reduced by $2^{N_P}/(N_P+1)$ times, which indicates that the computational complexity involved with the optimization can be exponentially simplified. Note that a progressive bitstream is typically transformed into a sequence of packets, in part because multiple levels of unequal error protection are required for the progressive transmission.

V. Numerical Evaluation and Discussion

We first numerically evaluate the outage probabilities and the uncoded BERs of OSTBC and SM with a ZF receiver for the same data rate. The error probabilities are evaluated in 2×4 MIMO systems for various data rates $R = 6$, 9, and 12 bits/s/Hz. The results are shown in Figs. 3 and 4, where solid curves denote the exact error probabilities, and dashed curves show the high SNR approximate error probabilities. Figs. 3 and 4 show that, for both the outage probabilities and the BERs, the gap between the approximate crossover point and the exact one becomes smaller as transmission data rate increases. For novel wireless communication systems targeting high data rates, the closed-form expressions of the approximate

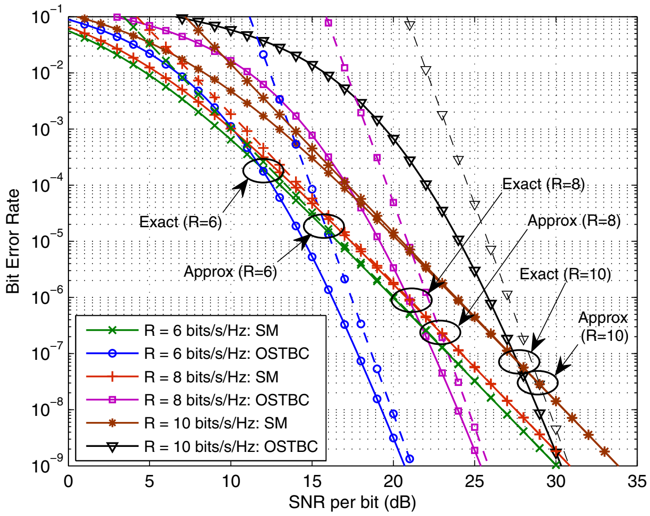

Fig. 4. The exact and high SNR approximate uncoded BERs of OSTBC and SM with a ZF receiver for 2×4 MIMO systems in i.i.d Rayleigh fading channels. Solid curves denote the exact BERs, and dashed curves do the high SNR approximate BERs. The exact and approximate crossover points are marked with circles.

crossover points, given by (4), (6), (15) and (16), will become more accurate. From Figs. 3 and 4, it is seen that as data rate increases, the crossover points for the outage probabilities as well as the uncoded BERs behave in a way predicted by the analysis given by (8) and (18) (refer to Fig. 1).

In Section IV, we presented the optimal space-time coding for the transmission of progressive sources. In the following, we will compare the performances of the optimal space-time coding and the suboptimal ones for progressive transmission. We evaluate the performances for 2×2 MIMO systems using the source coder SPIHT [16], and provide results for the standard 8 bits per pixel (bpp) 512×512 Lena image with a transmission rate of 0.5 bpp. We assume a slow fading channel, such that channel coefficients are nearly constant over an image, and the channel estimation at the receiver is perfect. The end-to-end performance is measured by the expected distortion of the image, denoted by $E[D]$.

We describe the evaluation of the expected distortion. The system takes a compressed progressive bitstream from the source encoder, and transforms it into a sequence of packets with error detection and correction capability. Then, as shown in Fig. 2, the packets are encoded by the space-time codes. At the receiver, if a received packet is correctly decoded, the next packet is considered by the source decoder. Otherwise, the decoding is terminated and the source is reconstructed from only the correctly decoded packets due to the nature of progressive source code. Let d_n denote the distortion of the source using the first n packets for the source decoder ($0 \leq n \leq N_P$), where N_P is the number of packets for an image. The d_n can be expressed as $d_n = D\left(\sum_{i=1}^{n} r_i\right)$, where r_i is the number of source bits in the ith packet ($1 \leq i \leq N_P$), and $D(x)$ denotes the operational distortion-rate function of the source. We also let $P_{e,n}$ denote the probability that no decoding errors occur in the first n packets with an error in the next one ($1 \leq n \leq N_P - 1$). Then, the expected distortion, $E[D]$, can be calculated from both d_n and $P_{e,n}$. Note that $E[D]$ is a function of the SNR as well as the transmission data rate and the space-time code that are assigned to each packet. Let C_i denote the space-time code assigned to ith packet ($1 \leq i \leq N_P$). One can find the optimal set of space-time codes, $\mathbf{C}_{opt} = [C_1, \cdots, C_{N_P}]_{opt}$, which minimizes the expected distortion over a range of average SNRs using the weighted cost function as follows:

$$\arg\min_{C_1,\cdots,C_{N_P}} \frac{\int_0^\infty \omega(\gamma_s) E[D] d\gamma_s}{\int_0^\infty \omega(\gamma_s) d\gamma_s} \tag{19}$$

where $w(\gamma_s)$ in [0, 1] is the weight function. For example, $w(\gamma_s)$ can be given by $\omega(\gamma_s) = u(\gamma_s - \gamma_s^A) - u(\gamma_s - \gamma_s^B)$, where $u(x)$ is the unit step function. Eq. (19) indicates that the $C_1, \cdots, C_{N_P}$ are chosen such that the sum of the expected distortion of the receivers distributed in the range of $\gamma_s^A \leq \gamma_s \leq \gamma_s^B$ is minimized. Note that the amount of computation involved in Eq. (19) exponentially grows as N_P increases. Alternatively, as presented in Section IV, we may choose the codes, $C_1, \cdots, C_{N_P}$, with the constraint that the $k+1$st, $k+2$nd, …, N_Pth packets should be encoded with SM (i.e., OSTBC is excluded) if the kth packet is encoded with SM.

To compare the image quality, we use the peak-signal-to-noise ratio (PSNR), defined as $10\log\frac{255^2}{E[D]}$ (dB). We evaluate the PSNR performance as follows: We first compute (19) using the expected distortion, $E[D]$, which is obtained from simulation, and the weight function, $w(\gamma_s)$, described below (19). Next, with the optimal set of codes, $\mathbf{C}_{opt} = [C_1, \cdots, C_{N_P}]_{opt}$, obtained from (19), we evaluate the PSNR over a range of SNRs, $\gamma_s^A \leq \gamma_s \leq \gamma_s^B$. In this evaluation, error correction coding is not considered. The performance is evaluated for the case when a sequence of 15 packets is transmitted (i.e., $N_P = 15$) as an example, and we assume that the transmission data rates are assigned in a manner such that $R_1 = R_2 = R_3 = 4$ (bits/s/Hz), $R_4 = R_5 = R_6 = 6$ (bits/s/Hz), $R_7 = R_8 = R_9 = 8$ (bits/s/Hz), $R_{10} = R_{11} = R_{12} = 10$ (bits/s/Hz), and $R_{13} = R_{14} = R_{15} = 12$ (bits/s/Hz), where R_i denotes the data rate employed by the ith packet. For this specific setup, the optimal set of space-time codes computed from (19) is given by $C_1 = C_2 = \cdots = C_6 = \text{OSTBC}$, and $C_7 = C_8 = \cdots = C_{15} = \text{SM}$. Fig. 5 shows the PSNR of such an optimal set of space-time codes, in addition to showing the PSNRs of other suboptimal sets of codes, such as the second best set of codes and the worst set of codes. Fig. 5 also shows the PSNR corresponding to the expected distortion that is averaged over all the possible sets of space-time codes (note that the number of possible sets of space-time codes is 2^{N_P}). From this example, it is seen that PSNR performance of the progressive source tends to be sensitive to the way space-time codes are assigned to a sequence of packets, due to the

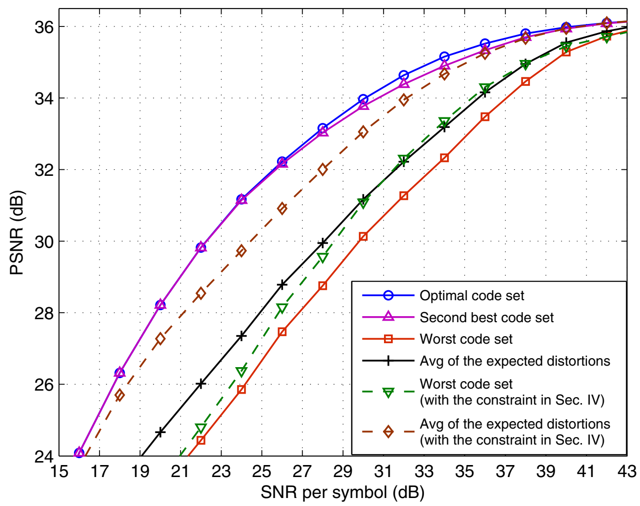

Fig. 5. The PSNR performance of the optimal set of space-time codes and suboptimal ones for the transmission of progressive 8 bpp 512×512 Lena image for 2×2 MIMO systems in i.i.d Rayleigh fading channels.

unequal transmission data rates and target error rates of the progressive bitstream.

Fig. 5 also shows the PSNR performance when (19) is computed with the constraint presented in Section IV (in this case, the number of possible sets of space-time codes is reduced to N_P+1). We note that the same optimal set of codes has been obtained when (19) is computed with and without the constraint. That is, without losing any PSNR performance, the computational complexity involved with the optimization can be reduced by exploiting the proof of the monotonic behavior of the crossover point, as shown in Fig. 1. It is also seen that the expected distortion, averaged over all the possible sets of space-time codes, gets better when the constraint in Section IV is introduced, which shows that, on the average, the constraint in Section IV is a good strategy for the space-time coding of progressive sources.

VI. Conclusions

Due to the differences of importance in the bitstream, when progressive multimedia are transmitted over MIMO channels, the tradeoff between the space-time codes should be clarified in terms of their target error rates and data rates. To address this matter, we analyzed the behavior of the crossover point of the error probability curves for OSTBC and SM with a ZF linear receiver. To make the analysis tractable, we explored the asymptotic regime of high SNR. The analytical results for the information outage probability and the uncoded BER coincided such that, as data rate increases, the crossover point in error probability monotonically decreases, whereas that in the SNR monotonically increases. We next showed that those analytical results can be used to simplify the computations involved with the optimal space-time coding of a sequence of numerous progressive packets. The work in this paper has significance in terms of its impact in the area of multimedia communications, and its analysis for the monotonic behavior of the crossover points.

References

[1] Y. Shen, P. C. Cosman, and L. B. Milstein, "Video coding with fixed length packetization for a tandem channel," *IEEE Trans. Image Process.*, vol. 15, pp. 273–288, Feb. 2006.

[2] S.-H. Chang, P. C. Cosman and L. B. Milstein, "Iterative channel decoding of FEC-based multiple description codes," *IEEE Trans. Image Process.*, vol. 21, no. 3, pp. 1138–1152, Mar. 2012.

[3] D. Taubman and M. Marcellin, JPEG2000: Image Compression Fundamentals, Standards, and Practice. Norwell, MA: Kluwer, 2001.

[4] H. Schwarz, D. Marpe, and T. Wiegand, "Overview of the scalable video coding extension of H.264/AVC," *IEEE Trans. Circuits Syst. Video Technol.*, vol. 17, no. 9, pp. 1103–1120, Sept. 2007.

[5] V. Tarokh, H. Jafarkhani, and A. R. Calderbank, "Space-time block codes from orthogonal designs," *IEEE Trans. Info. Theory*, vol. 45, no. 5, pp. 1456–1467, July 1999.

[6] G. J. Foschini, "Layered space-time architecture for wireless communication in a fading environment when using multiple antennas," *Bell Labs. Tech. J.*, vol. 1, no. 2, pp. 41–59, 1996.

[7] A. Forenza, M. R. McKay, A. Pandharipande, R. W. Heath Jr., and I. B. Collings, "Adaptive MIMO transmission for exploiting the capacity of spatially correlated channels," *IEEE Trans. Veh. Technol.*, vol. 56, no. 2, pp. 619–630, Mar. 2007.

[8] A. Forenza, M. R. McKay, I. B. Collings, and R. W. Heath Jr., "Switching between OSTBC and spatial multiplexing with linear receivers in spatially correlated MIMO channels," in *Proc. IEEE VTC*, Melbourne, Australia, May 2006.

[9] S.-H. Chang, M. Rim, P. C. Cosman and L. B. Milstein, "Superposition MIMO coding for the broadcast of layered sources," *IEEE Trans. Commun.*, vol. 59, no. 12, pp. 3240–3248, Dec. 2011.

[10] K. Raj Kumar, G. Caire, and A. L. Moustakas, "Asymptotic performance of linear receivers in MIMO fading channels," *IEEE Trans. Info. Theory*, vol. 55, no. 10, pp. 4398–4418, Oct. 2009.

[11] K. Cho and D. Yoon, "On the general BER expression of one- and two-dimensional amplitude modulations," *IEEE Trans. Commun.*, vol. 50, no. 7, pp. 1074–1080, July 2002.

[12] S.-H. Chang, "Joint optimization of physical and application layers for wireless multimedia communications," Ph.D. dissertation, University of California, San Diego, 2010.

[13] S.-H. Chang, P. C. Cosman and L. B. Milstein, "Optimal transmission of progressive sources based on the error probability analysis of SM and OSTBC," *IEEE Trans. Veh. Technol.*, accepted for publication.

[14] C. Oestges and B. Clerckx, *MIMO Wireless Communications*, Orlando, FL: Academic, 2007.

[15] A. Hedayat and A. Nosratinia, "Outage and diversity of linear receivers in flat-fading MIMO channels," *IEEE Trans. Signal Process.*, vol. 55, no. 12, pp. 5868–5873, Dec. 2007.

[16] A. Said and W. A. Pearlman, "A new, fast, and efficient image codec based on set partitioning in hierarchical trees," *IEEE Trans. Circuits Syst. Video Technol.*, vol. 6, pp. 243–249, June 1996.